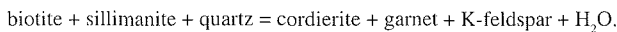


Cordierite in the Shackleton Range, Antarctica: First Recorded Occurrence

By Wolfgang Schubert* and Martin Olesch**

Summary: An example of cordierite-bearing gneiss that is part of a high-grade gneiss-migmatite sequence is described from the Hatch Plain in the Read Mountains of the Shackleton Range, Antarctica, for the first time. The cordierite-bearing rocks constitute the more melanosome portions of the metatectonic and migmatitic rocks that are associated with relict granulite facies rocks such as enderbitic granulite and enderbitic garnet granulite. The predominant mineral assemblage in the cordierite-bearing rocks is chemically homogeneous cordierite ($X_{Mg} 0.61$) and biotite ($X_{Mg} 0.47$), strongly zoned garnet ($X_{Mg} 0.18-0.11$), sillimanite, K-feldspar ($Or_{81-94} Ab_{5-18} An_{0-6}$), plagioclase (An_{28}), and quartz. Inclusions of sillimanite and biotite relics in both garnet and cordierite indicate that garnet and cordierite were produced by the coupled, discontinuous reaction



Various garnet-biotite and garnet-cordierite geothermometers and sillimanite-quartz-plagioclase-garnet-cordierite geobarometers yield a continuous clockwise path in the P-T diagram. The P-T conditions for equilibrium between garnet core and cordierite and between garnet core and biotite during peak metamorphism and migmatization were estimated to be 690 °C at 5-6 kb. This was followed by cooling and unloading with continuously changing conditions down to 515 °C at 2-3 kb. This low-pressure re-equilibration correlates with the pressure conditions evaluated by SCHULZE (1989) for the widespread granitic gneisses of the Read Group in the Shackleton Range. The associated relict enderbitic granulites representing low-pressure type granulite (8 kb; 790 °C) are comparable to similar low-pressure granulites from the East Antarctic craton. They were either formed by under-accretion processes after collision (WELLS 1979, p. 217) or they are a product of remetamorphism at P-T conditions intermediate between granulite and amphibolite facies. A model of a multiple imbrication zone with crustal thickening (CUTHBERT et al. 1983) is discussed for the formation of the relict granulites of the central and eastern Read Mountains which show higher pressure conditions (8-12 kb, SCHULZE & OLESCH 1990), indicating a Proterozoic crustal thickness of at least 40 km.

Zusammenfassung: Die Du Toit Nunataks in den Read Mountains der Shackleton Range, Antarktis, werden in ihrem metamorphen Anteil von hochgradigen Biotit-Granatgneisen, Amphiboliten und Migmatiten aufgebaut, welche lokal mit relikтив erhaltenen enderbitischen Granuliten und enderbitischen Granatgranuliten verzaht sind. Im Gebiet der Hatch Plain wurde darüber hinaus zum ersten Mal in der gesamten Shackleton Range Cordierit gefunden. Der Cordierit tritt vorwiegend im Melanosom der metatektisch ausgebildeten Sillimanit-Granat-Cordieritgneise auf. Die weitverbreitete Mineralparagenese ist hier Biotit ($X_{Mg} 0.47$), Cordierit ($X_{Mg} 0.61$) und stark zonarer Granat ($X_{Mg} 0.18-0.11$), neben Sillimanit, Kalifeldspat ($Or_{81-94} Ab_{5-18} An_{0-6}$), Plagioklas (An_{28}) und Quarz. Detailstudien an reliktischen Einschlüssen von Sillimanit und Biotit in Cordierit und in Granat belegen die Bildung von Granat und Cordierit über die gekoppelte, divariante Reaktion $\text{Biotit} + \text{Sillimanit} + \text{Quarz} = \text{Granat} + \text{Cordierit} + \text{Kalifeldspat} + H_2O$. P-T-Abschätzungen aufgrund verschiedener Granat-Biotit- und Granat-Cordierit-Thermometer, sowie von Sillimanit-Plagioklas-Quarz-Granat-Cordierit-Barometern ergaben einen kontinuierlichen

Pfad im Uhrzeigersinn im P-T-Diagramm. Die Gleichgewichtseinstellungen Granatkern - Biotit und Granatkern - Cordierit ergaben für den Höhepunkt der Metamorphose und Migmatitisierung Bedingungen von 690 °C/5-6 kb. Diese Bedingungen wurden durch Abkühlung, gekoppelt mit Entlastung stetig vermindert bis auf 515 °C/2-3 kb. Diese letztgenannten Niedrigdruckbedingungen der Cordieritgneise entsprechen den gleichen Drucksituationen, wie sie von SCHULZE (1989) für die weitverbreiteten gneissic granites der Read Gruppe in der Shackleton Range ermittelt wurden. Mit den Cordieritgneisen und Amphiboliten vergesellschaftete reliktische enderbitische Granulite repräsentieren Niedrig-Druck-Granulite mit Bildungsbedingungen um 8 kb und 790 °C. Sie sind mit ähnlichen Niedrig-Druck-Granuliten der Ostantarktis vergleichbar. Ihre Bildung würde entweder während eines Prozesses der Unter-Akkretion nach Kollision (WELLS 1979) vollzogen worden sein, oder ihre P-T-Bedingungen waren Hinweise auf einen erneuten Prozess einer Gleichgewichtseinstellung zwischen Granulit- und Amphibolitfazies. Die reliktischen Granulite der mittleren und östlichen Read Mountains, die höhere Druckbildungen anzeigen (SCHULZE & OLESCH 1990), werden als Bildungen in Zusammenhang mit Subduktion-Kollision, sowie wiederholten Einschüppungsprozessen nach CUTHBERT et al. (1983) diskutiert.

DISTRIBUTION OF LITHOLOGIES

The southern, older part of the Shackleton Range (Read Mountains) is formed by the Shackleton Range Metamorphic Complex (CLARKSON 1972, 1982). It consists of metamorphic basement rocks of Proterozoic age (PANKHURST et al. 1983, HOFMANN & PAECH 1983).

Gneissic granite

The metamorphic rocks of the Read Mountains area (Read Group) are dominated by weakly foliated gneissic igneous bodies derived from intrusive granites, the so-called „gneissic granite“ of CLARKSON (1972, 1982) and PANKHURST et al. (1983). These gneissic granites are coarse- to medium-grained orthogneisses with the more massive texture in the central parts of the outcrops changing to a more foliated texture in the outer parts. They contain quartz, microcline, plagioclase (An_{27-30}), muscovite, pale green biotite, accessory sillimanite and in parts almandine-rich garnet.

In the foliated gneissic parts, the texture is dominated by heavily sericitized feldspars, chloritized biotite and mosaics of strained quartz. Analytical data for garnet indicate only weak zoning with core compositions of $Alm_{84.3} Prp_{8.6} Grs_{4.4} Sps_{2.4}$ and rim compositions of $Alm_{87.0} Prp_{6.0} Grs_{3.3} Sps_{3.3}$ (SCHULZE 1989).

* Prof. Dr. Wolfgang Schubert, Institut für Mineralogie, Universität Würzburg, Am Hubland, D-97074 Würzburg, Germany.

** Prof. Dr. Martin Olesch, Fachbereich Geowissenschaften, Universität Bremen, Postfach 330440, D-28334 Bremen, Germany.

Manuscript received 24 November 1993; accepted 24 December 1994

Some of the contacts between the granite gneiss and the surrounding metamorphic country rocks are fault or thrust planes (Fig. 2).

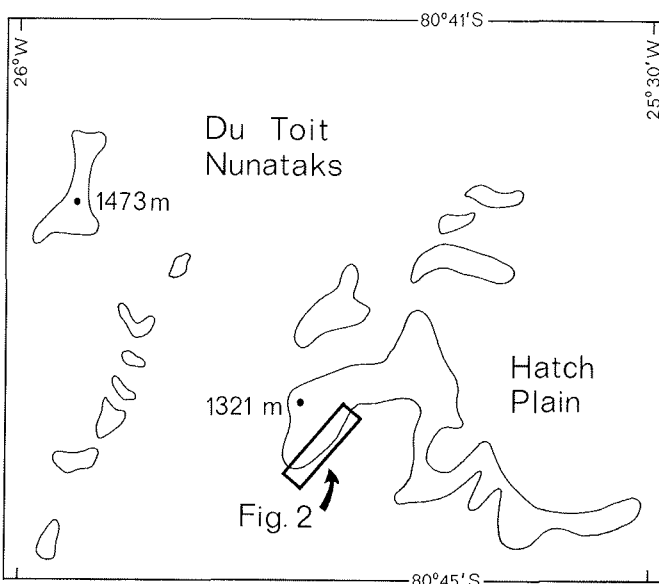


Fig. 1: Location map of the study area in the western Read Mountains, Shackleton Range, Antarctica.

Abb.1: Übersichtskarte des Untersuchungsgebietes in den westlichen Read Mountains, Shackleton Range, Antarktis.

Metamorphics

The gneissic granite is associated with medium- to high-grade metamorphic rocks of metapelitic, metabasic, metaquartzitic and metacarbonate composition, as well as migmatites, all cut by irregular aplitic to pegmatitic veins and networks of veins of granitic composition. An excellent example of this great variety of metamorphic rocks can be studied in the outcrops and cirques at the Du Toit Nunataks (Fig. 1), where detailed mapping of the NE-SW scarp just west of Hatch Plain revealed the variety of associated rock types and their complex spatial relationships (Fig. 2).

The metamorphic rocks comprise widespread garnet-biotite gneiss and metatectic garnet gneiss, biotite amphibolite, zoisite-biotite amphibolite, marble, silicate marble and migmatite. Detailed petrographic information on these rocks has been published by CLARKSON (1982).

Relict granulite facies basement gneiss associated with the amphibolite was found in the southwestern part of the NE-SW scarp, west of Hatch Plain. Using the nomenclature of WINKLER (1979) (but not following his proposal to use „granolite“ in stead of „granulite“), this gneiss can be termed enderbitic granulite and enderbitic garnet granulite. These rocks are medium-grained, massive to discontinuously striped, unusually dense, mesocratic and contain the characteristic granulite facies mineral assemblage: orthopyroxene (X_{Mg} 0.40), quartz, garnet (X_{Mg} 0.15), biotite (X_{Mg} 0.41), plagioclase (An_{46}), K-feldspar, and

secondary cummingtonite (X_{Mg} 0.42) and Ca-amphibole (X_{Mg} 0.44).

Detailed information about the petrography, mineral chemistry and petrology of these granulite facies rocks is given in SCHUBERT & WILL (1994). The following discussion will concentrate on the newly found cordierite-bearing gneiss.

SILLIMANITE-GARNET-CORDIERITE GNEISS

Cordierite-bearing rocks were found within the metatectic garnet gneiss complex in the outcrop west of Hatch Plain (Fig. 2). This is the first finding of cordierite in the Shackleton Range. These sillimanite-garnet-cordierite gneisses are at 80° 43.5' S, 25° 45' W (U.S. GEOL. SURV. 1983). In the field, the cordierite gneiss is closely associated with high-grade migmatites which show a stromatic to phlebitic structure due to migmatitic differentiation. The contact between mafic and felsic parts of the migmatites is irregular and the leucosomes often appear to swirl and are discontinuous.

The fresh sillimanite-garnet-cordierite gneiss is dark bluish grey with metamorphic banding ranging in thickness of 1-5 cm. The mineral fabric comprises slightly deformed layers of interleaved or parallel flakes of biotite, which describe a wavy lenticular structure around coarse-grained cordierite, garnet and feldspars.

Migmatization of the sillimanite-garnet-cordierite gneiss has differentiated it into melanosome and coarser grained leucosome. The mafic, cordierite-rich parts comprise reddish-brown biotite, garnet, microcline perthite and minor plagioclase (An_{28}), quartz, and accessories.

Prismatic sillimanite I is generally, but not always present. It occurs intimately intergrown with biotite following the gneissic fabric. The reaction producing sillimanite I appears to involve breakdown of biotite. Late-kinematic sillimanite II occurring as ropes and mats of fibrolite indicates the formation of a second sillimanite generation.

A representative modal composition of sample W-173 is 28 vol.% biotite, 12 % cordierite, 6 % garnet, 3 % sillimanite, 3 % K-feldspar, 36 % plagioclase, 11 % quartz, and 1 % accessories. The mineral content and the relative volume of leucosome are rather variable. The main constituents are K-feldspar, plagioclase and quartz (undulatory extinction); garnet, biotite and some cordierite may be present in variable amounts, primary muscovite is absent.

The colourless cordierite, where fresh, forms elongated untwinned porphyroblasts with a very light yellow interference colour. Cordierite and plagioclase contain relict inclusions of prismatic sillimanite or very rarely corundum. Relict sillimanite is arranged in helicitic or linear inclusion trails (Fig. 3); whereas the core of cordierite is full of sillimanite needles, the rim is free of

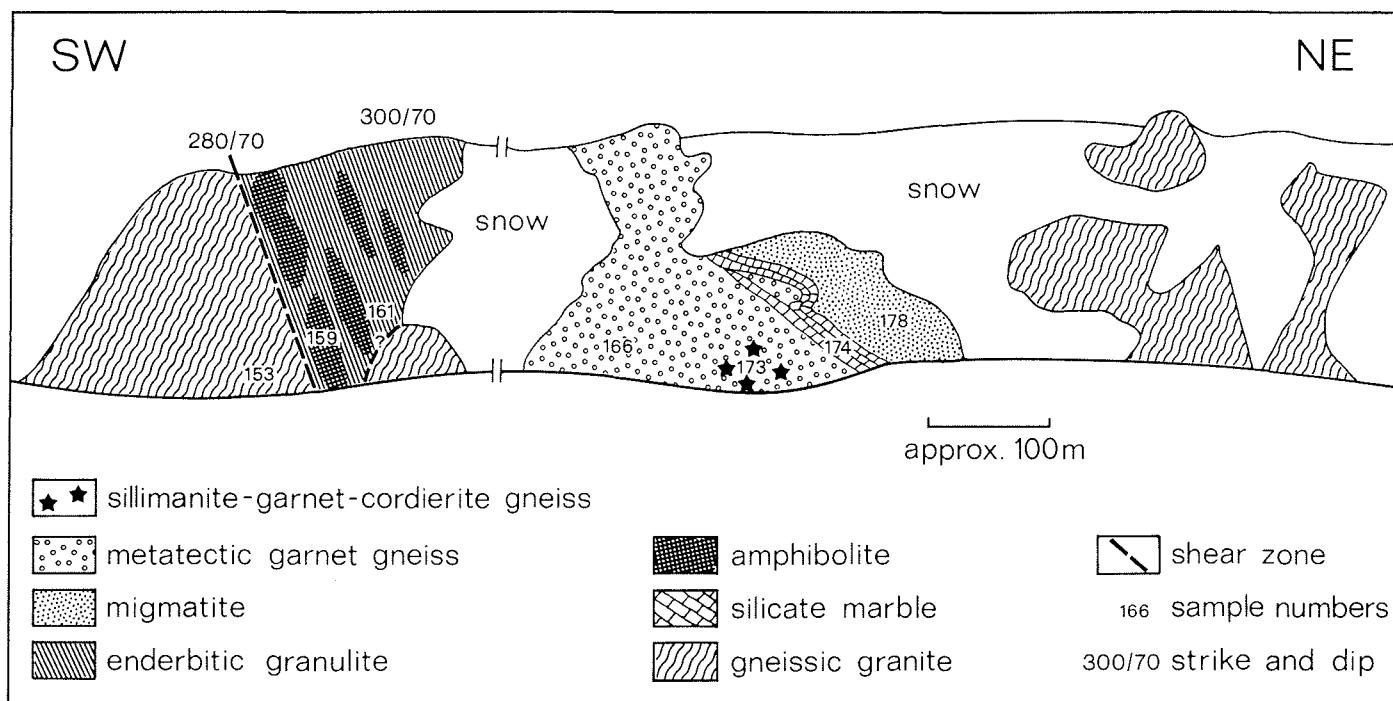


Fig. 2: Geological map of the NE-SW scarp west of Hatch Plain, Du Toit Nunataks in the Shackleton Range. The locations of the sillimanite-garnet-cordierite gneiss are marked by asterisks. The approximate height of the scarp is 120 m.

Abb. 2: Geologische Karte der NE-SW-Wand westlich Hatch Plain in den Du Toit Nunataks, Shackleton Range. Die Fundstellen des Sillimanit-Granat-Cordieritgneises sind durch Sternchen markiert. Die Wandhöhe beträgt ca. 120 m.

inclusions. Inclusions of biotite in cordierite are also visible, separate from the sillimanite inclusions. Thus, cordierite is in contact with biotite and a quartz-two feldspar matrix.

Garnet forms embayed, sometimes elongated, xenoblastic porphyroblasts up to 5 mm in diameter or concentrations of smaller grains together with biotite in the matrix. It shows pronounced pre-kinematic, subparallel cracks filled with Fe-prochlorite (optical determination) and secondary white mica.

Some garnets are poor in quartz and biotite inclusions, others appear poikiloblastic, hosting helicitic inclusion trails of sillimanite. This relict sillimanite retains its original arrangement in the matrix of the gneiss (Fig. 4). Some inclusions of relict biotite are also visible, but also in this case, no contacts between sillimanite and biotite were observed.

Plagioclase is mostly fresh with narrow albite and pericline lamellae and a composition around An₂₈. K-feldspar appears as unexsolved microcline with 94 mol% orthoclase and as orthoclase with microperthite exsolution flames with a lower orthoclase content of 81 to 89 mol%.

The grain size of the quartz varies considerably due to late-tectonic deformation. It shows strong undulatory extinction, is often blastomylonitic or recrystallized at grain boundaries.

In general, the minerals of the sillimanite-garnet-cordierite gneiss are fresh, but retrograde changes include some pinitization of cordierite, sericitization of feldspars, oxidation of biotite, and growth of secondary chlorite and white mica.

Whole-rock and mineral chemistry

Bulk-rock analyses of sillimanite-garnet-cordierite gneiss from the Du Toit Nunataks yield intermediate SiO₂ values (51.4 wt.%), high Al₂O₃ (21.7 wt.%), high FeO (10.5 wt.%), and high FeO/(FeO+MgO) (0.73). Thus, these rocks represent a „clayey graywacke“ protolith according to the geochemical classification scheme of WIMMENAUER (1984). Microprobe analyses were carried out with a CAMEBAX SX 50 and are presented in Tabs. 1 and 2. The acceleration voltage was 15 kV, beam current 10 nA, the matrix correction was made using the CAMECA PAP program. A summary of mineral chemistry will be presented below, additional analytical data can be obtained from the authors on request.

Cordierite

Representative microprobe analyses of cordierite are given in Tab. 1. The sum of cations per 18 oxygens is close to the theo-

retical value of 11.00 (11.00-11.02). The totals of 97.51 to 97.67 wt.% are consistent with the optical properties and suggest moderate to high contents of volatiles in the lattice channels (ARMBRUSTER & BLOSS 1982). The negative optic sign of the cordierite suggests a low content of CO₂ in the channel-filling fluid. The sodium content is low, with total alkalis rarely exceeding 0.079 cations per formula unit. The cordierite compositions yield a mean X_{Mg} of 0.61-0.62, and there is no zoning or elevated X_{Mg} adjacent to garnet and biotite.

Garnet

Garnet shows the widest range of X_{Mg} of all of the analyzed minerals. Representative microprobe data are given in Tab. 1. Garnets from the melanosome of the sillimanite-garnet-cordierite gneiss belong essentially to the almandine-pyrope solid solution series, with a mean core composition of Alm₇₈Prp₁₇Gro_{2.6}Sps_{2.2}. The composition of garnet in contact with biotite is Pyr_{10.6}Alm_{82.7}Grs_{2.6-2.7}Sps_{4.0}. Thus, compositional

Sample Comment	Biotite			Garnet			Cordierite	
	W-168	W-173 rim	W-173 core	W-168 rim	W-173 rim	W-173 core	W-168	W-173
SiO ₂	35.19	35.10	36.81	36.53	36.96	36.61	48.05	48.18
TiO ₂	2.93	3.47	3.34	0	0.04	0.04	0.05	0.03
Al ₂ O ₃	18.84	18.91	18.88	21.73	20.61	21.12	32.78	32.94
Cr ₂ O ₃	0.10	0.07	0.07	0.12	0.09	0	n.d.	n.d.
MgO	10.23	9.48	9.33	2.81	2.64	4.35	7.52	7.75
CaO	0	0	0.01	1.07	0.96	0.92	0.06	0.01
MnO	0	0	0.05	1.83	1.76	0.99	0.07	0.14
FeO	19.36	18.93	19.24	36.71	37.61	35.25	8.60	8.30
Na ₂ O	0.23	0.09	0.08	n.d.	n.d.	n.d.	0.38	0.30
K ₂ O	9.27	9.65	9.64	n.d.	n.d.	n.d.	0.02	0.01
Total	96.15	96.70	97.44	100.80	100.67	99.28	97.53	97.66
no. of O	22	22	22	24	24	24	18	18
Si	5.286	5.396	5.458	5.876	5.967	5.920	4.999	4.997
Al ⁴	2.714	2.604	2.542	0.124	0.033	0.080	1.001	1.003
	8	8	8	6	6	6	6	6
Al ⁶	0.621	0.728	0.757	3.996	3.888	3.944	3.018	3.022
Ti	0.331	0.390	0.372	0	0.005	0.006	0.004	0.003
Cr	0.012	0.009	0.009	0.014	0.012	0	n.d.	n.d.
Fe ³⁺					0.095	0.050		
Mg	2.290	2.113	2.061	0.674	0.636	1.049	1.166	1.199
Ca	0	0	0.001	0.185	0.167	0.159	0.006	0.001
Mn	0	0	0.007	0.250	0.241	0.136	0.006	0.012
Fe ²⁺	2.432	2.367	2.386	4.938	4.983	4.723	0.748	0.720
Na	0.067	0.026	0.024	n.d.	n.d.	n.d.	0.076	0.060
K	1.777	1.839	1.823	n.d.	n.d.	n.d.	0.003	0.002
Total	15.53	15.47	15.44	16.06	16.03	16.07	11.03	11.02
X _{Mg}	0.49	0.47	0.46	0.12	0.11	0.18	0.61	0.62
X _{Fe}	0.51	0.53	0.54	0.88	0.89	0.82	0.39	0.38
pyrope mol%				11.1	10.6	17.3		
almandine mol%				81.7	82.7	77.9		
spessartine mol%				4.1	4.0	2.2		
grossular mol%				3.1	2.7	2.6		

Tab. 1: Representative electron-microprobe analyses of biotite, garnet and cordierite from sillimanite-garnet-cordierite gneiss samples W-168 and W-173, Du Toit Nunataks, Read Group, Shackleton Range, Antarctica. Oxide weight %.

Tab. 1: Repräsentative Mikrosonden-Analysen von Biotit, Granat und Cordierit aus Sillimanit-Granat-Cordieritgneis-Proben W-168 und W-173, Du Toit Nunatakk, Gead-Gruppe, Shackleton Range, Antarktis. Oxid-Gew.%.

changes towards neighbouring biotite are characterized by a strong decrease in pyrope content, an increase in almandine, and only a small change in spessartine. The calcium content remains nearly constant.

Fig. 6 shows the typical zoning of a garnet grain 3 mm in diameter bordered by biotite on both sides and set in a cordierite-bearing melanosome. The bell-shaped form of the Fe, Mg and Mn curves is obvious. The Fe content steadily rises from 4.76 in the core to 5.09 at the rim and the Mn content from 0.129 to 0.270. The increasing Fe/Mg ratio from the core to the grain rim indicates a decrease in temperature (RAHEIM 1975, PERCHUK 1977). The rim of garnet W-173 shows a deficiency of 0.095 Al per formula unit in the octahedral position, which is compensated for by Ti and Cr. It therefore seems reasonable to suggest that a considerable amount of andradite (up to 1.8 mol%) is present in the garnet rim of sample W-173.

Biotite

Tab. 1 shows representative microprobe analyses of biotites from samples W-168 and W-173. In the absence of measured data of H₂O contents, the structural formulae have been calculated on the basis of 22 oxygens. Several dozen analyses were carried out to check for possible zoning in biotite. The chemical composition of the analyzed biotites is relatively uniform, however. No striking differences between core and rim compositions were found (e.g. core and rim compositions of sample W-173 in Tab. 1). The totals for biotite analyses range between 96.70 and 97.44 wt.%, owing to the lack of H₂O determinations. X_{Mg} is uniformly 0.46 - 0.47, Ti is generally high (3.34-3.47 wt.% TiO₂), and high K/(K+Na) values of biotites are typical for high-grade metamorphism (DYYMEK 1983). The composition of biotites in the analyzed garnet-cordierite gneiss samples plots on the ideal biotite plane annite-phlogopite-side-trophyllite-eastonite (Fig. 7). The data compiled by GUIDOTTI (1984) were used to define the fields for biotite in the upper amphibolite to granulite-grade metapelites for comparison. Our biotite analyses plot within the field of the upper amphibolite to granulite-grade metapelites. Biotites from neighbouring enderbitic granulite show considerably lower Al^{VI}, plotting close to GUIDOTTI's (1984) base line of the biotite plane of biotites from granulite-grade metapelites, but with slightly lower X_{Mg} values (factor 0.7).

Feldspars

Analyses of fresh albite-twinned plagioclase yielded an average anorthite content of 28 mol% with a range from 27-29 %. Clear zoning was not detected. Orthoclase contents in plagioclase are low and range from 0.6-1.2 mol% in sample W-173. Representative microprobe analyses of coexisting feldspars are given in Table 2. K-feldspar analyses vary more because of exsolution. Microscopically unexsolved microcline is

Sample	Oxide weight %					
	plagioclase	perthite	K-feldspar	micro-cline		
W-168	W-173	W-173	W-168	W-173	W-169	
SiO ₂	60.13	61.56	68.74	62.71	64.13	64.89
Al ₂ O ₃	25.11	24.45	20.27	18.90	19.02	18.49
FeO	0	0.02	0.09	0.03	0.04	0.03
CaO	5.94	5.67	0.33	0.08	0.13	0.01
BaO	0.02	0	0.07	0.38	0.40	0.03
Na ₂ O	7.85	8.21	9.26	0.51	1.97	0.35
K ₂ O	0.14	0.14	2.74	14.51	13.52	15.86
Total	99.19 ¹⁾	100.05	101.50	99.12 ²⁾	99.21	99.66 ³⁾
no. of O	8	8	8	8	8	8
Si	2.690	2.729	2.986	2.970	2.969	2.997
Al	1.324	1.277	1.014	1.054	1.038	1.006
Fe ²⁺	0	0.001	0.004	0.001	0.004	0.001
Ca	0.285	0.269	0.015	0.004	0.007	0.001
Ba	0.001	0	0	0.007	0.007	0.001
Na	0.681	0.705	0.762	0.047	0.177	0.031
K	0.008	0.008	0.149	0.877	0.799	0.934
Total	4.989	4.989	4.929	4.960	4.999	4.971
Or	0.8	0.8	16.0	94.4	81.3	96.7
ab	70.0	71.8	82.4	5.1	18.0	3.2
an	29.2	27.4	1.6	0.5	0.7	0.1

Tab. 2: Representative microprobe analyses of feldspars. ¹⁾in addition MnO 0.10 wt.%; ²⁾in addition MnO 0.11 wt.%; ³⁾in addition MnO 0.03, ZnO 0.28 wt.%

Tab. 2: Repräsentative Mikrosonden-Analysen von Feldspäten.

Or₉₄Ab₅An_{0.5} (sample W-168). K-feldspar with flame-like microperthite shows a wider composition range of Or₈₁₋₈₉Ab₁₈₋₁₀An_{0.4-0.7}, while the exsolved albite itself shows Or₁₆Ab₈₂An_{1.6}. In the microcline pegmatite (sample W-169) associated with the garnet-cordierite gneiss, the K-feldspar composition is Or₉₇Ab₃An_{0.1}; the means of 20 K-feldspar analyses of the same sample are Or_{95.5±2.2}Ab_{4.2±1.7}An_{0.3±0.3}.

Mineral assemblages and reactions

The following mineral assemblage was observed in the leucosome of the sillimanite-garnet-cordierite gneiss:

K-feldspar - plagioclase - quartz ± biotite ± cordierite ± garnet

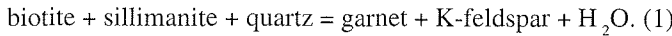
The stable mineral assemblage of the melanosome of the sillimanite-garnet-cordierite gneiss is represented by

cordierite - biotite - garnet - sillimanite - plagioclase ± K-feldspar ± quartz.

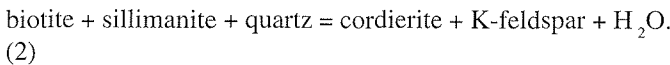
Prograde reactions

To obtain some information about the mineral-forming reactions which can be recognized in the sillimanite-garnet-cordierite gneiss, the following observations are important:

- (a) Garnet and cordierite are in contact with biotite, two feldspars and quartz.
- (b) Both garnet and cordierite contain numerous relict inclusions of sillimanite.
- (c) When biotite (scarce) is preserved as an inclusion in garnet it is spatially separated from the sillimanite inclusions. Thus, garnet was formed according to the following prograde reaction:



Cordierite grains surrounded by biotite laths are found to have cores full of sillimanite inclusions and peripheries poor in sillimanite, indicating that here too, biotite and sillimanite are the reacting phases and cordierite is the reaction product. Thus, on the basis of textural criteria, the prograde formation of cordierite is attributed to the reaction



Some observations suggest that reaction (2) did not completely move to the right side: Sillimanite-free haloes around biotite (BLÜMEL 1978) are not developed in all cases, and the peripheries of cordierite bordering biotite are not always devoid of sillimanite (BLÜMEL & SCHREYER 1977). There are two possible, interrelated reasons why reaction (2) to the right is incomplete:

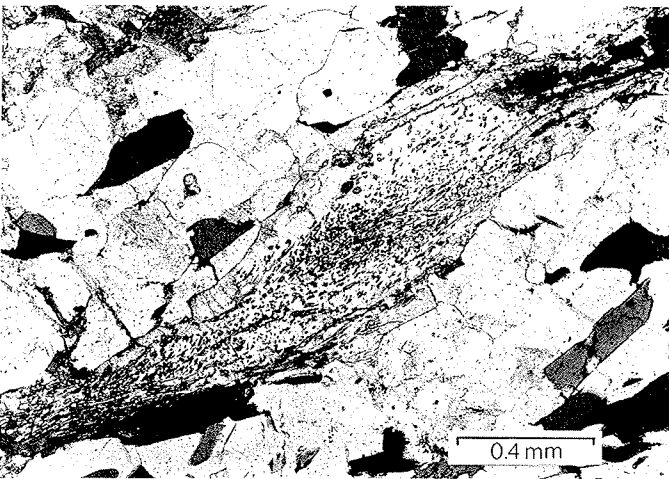


Fig. 3: Cordierite producing reaction $\text{bio} + \text{sill} + \text{qu} = \text{cord} + \text{K-fsp} + \text{H}_2\text{O}$. Cordierite is rimmed by biotite and shows inclusion trails of sillimanite needles. Note the sillimanite-free periphery of cordierite in some parts where it borders biotite. Sillimanite-garnet-cordierite gneiss, sample W-167, plane-polarized light.

Abb. 3: Cordieritbildende Reaktion $\text{Bio} + \text{Sill} + \text{Qu} = \text{Cord} + \text{Kfsp} + \text{H}_2\text{O}$. Cordierit ist von Biotit umgeben und zeigt Einschlüssebahnen von Sillimanitnadeln. Beachte die Sillimanit-freien Randbereiche des Cordierits wo er an Biotit grenzt. Sillimanit-Granat-Cordieritgneis, Probe W-167, einfach polarisiertes Licht.

(a) The absence of quartz in mafic parts of the cordierite gneiss suggests that - due to complete consumption of quartz - reaction (2) was blocked before all the sillimanite and biotite had reacted to form cordierite. This is further supported by the observation that those bands in the foliated gneiss made up of biotite-sillimanite do not contain cordierite. This mineral developed only when quartz was also present in the bands.



Fig. 4: Part of a porphyroblastic garnet (grey, high relief) including some biotite (darker grey, lower right) and quartz. The garnet is in contact with cordierite (upper part of the photo). Sillimanite needles follow the primary gneissic fabric and are visible in both garnet and cordierite. Subparallel cracks in garnet are filled with secondary chlorite and white mica. Sillimanite-garnet-cordierite gneiss, sample W-167, plane-polarized light.

Abb. 4: Teil eines porphyroblastischen Granats (graue, hohes Relief) mit Einschlüssen von Biotit (dunkler grau, unten rechts) und Quarz. Der Granat ist mit Cordierit in Kontakt (oberer Teil der Abb.). Die Sillimanitnadeln folgen dem primären Gneisgefüge und sind sowohl in Granat als auch in Cordierit sichtbar. Auf subparallelen Rissen im Granat wächst sekundärer Chlorit und Hellelglimmer. Sillimanit-Granat-Cordieritgneis, Probe W-167, einfach polarisiertes Licht.

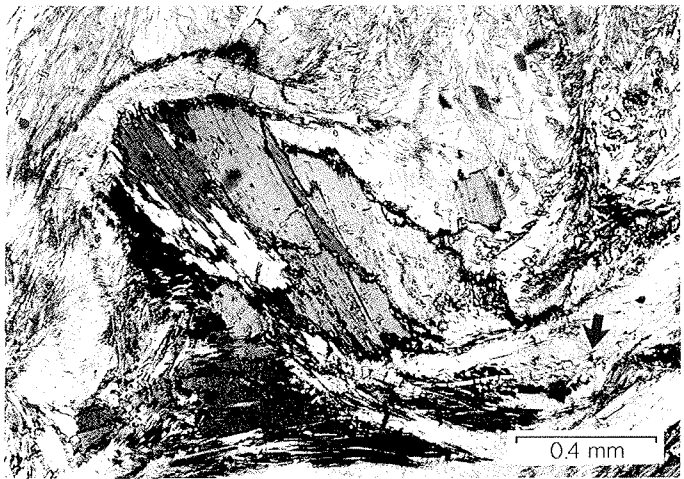


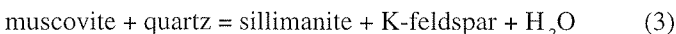
Fig. 5: Ropes of late-kinematic sillimanite II (fibrolite) replacing central biotite at its upper left and lower right end. A kinked sillimanite I prism (arrow) is still preserved in sillimanite II (fibrolite). Cordierite filled with sillimanite I inclusions (upper right). Sillimanite-garnet-cordierite gneiss, sample W-168, plane-polarized light.

Abb. 5: Stränge von spätkinematischem Sillimanit II (Fibrolith), der den zentralen Biotit an seinem oberen linken und unteren rechten Ende ersetzt. Ein verknicktes Prisma von Sillimanit I (Pfeil) ist noch im Sillimanit II (Fibrolith) erhalten. Cordierit ist gefüllt mit Einschlüssen von Sillimanit I (oben rechts). Sillimanit-Granat-Cordieritgneis, Probe W-168, einfach polarisiertes Licht.

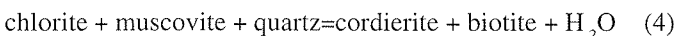
(b) This mechanism was probably accelerated by removal of quartz from the melanosome during advanced migmatization. In biotite-rich portions of the gneiss, highly deformed mats of sillimanite II (fibrolite) represent a second generation of aluminum silicate, showing inclusions of small corroded biotite and prismatic sillimanite I (Fig. 5).

Retrogressive reactions

Tiny muscovite flakes often appear as alteration products surrounding sillimanite/fibrolite crystals. Widespread pinitization of cordierite leads to the growth of secondary white mica along cracks, gradually replacing cordierite, coupled with growth of younger Fe-prochlorite (optical determination). The alteration observed in thin section indicates that the stability field of muscovite and quartz and that of chlorite, muscovite and quartz are defined by the following reactions (BIRD & FAWCETT 1973):



and



Phase petrology

In the analyzed cordierite gneiss, no primary muscovite is stable with quartz. On the basis of the data in the foregoing chapter, coexisting mineral phases can be plotted in the usual AFM diagram using K-feldspar as the point of projection.

In the AFM diagram, zoning in garnet is indicated by representative rim and core compositions. No zoning was detected in biotite. The entire range of compositional variation of the biotite analyses for samples W-168 and W-173 (melanosomic parts of sillimanite-garnet-cordierite gneiss) is marked by a bar in Figure 8.

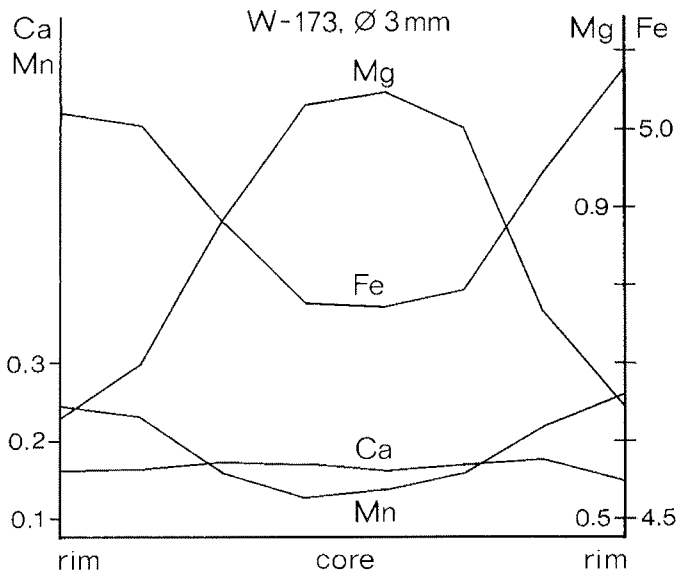


Fig. 6: Zoning in garnet from sillimanite-garnet-cordierite gneiss sample W-173. Cations per formula unit Ca, Mn, Mg, and Fe are plotted as a function of distance along a 3 mm traverse across a single inclusion-free garnet grain.

Abb. 6: Zonarbau von Granat aus Sillimanit-Granat-Cordieritgneis, Probe W-173. Die Kationen pro Formeleinheit Ca, Mn, Mg und Fe sind dargestellt entlang einer 3 mm Traverse durch ein einzelnes, einschlußfreies Granatkorn.

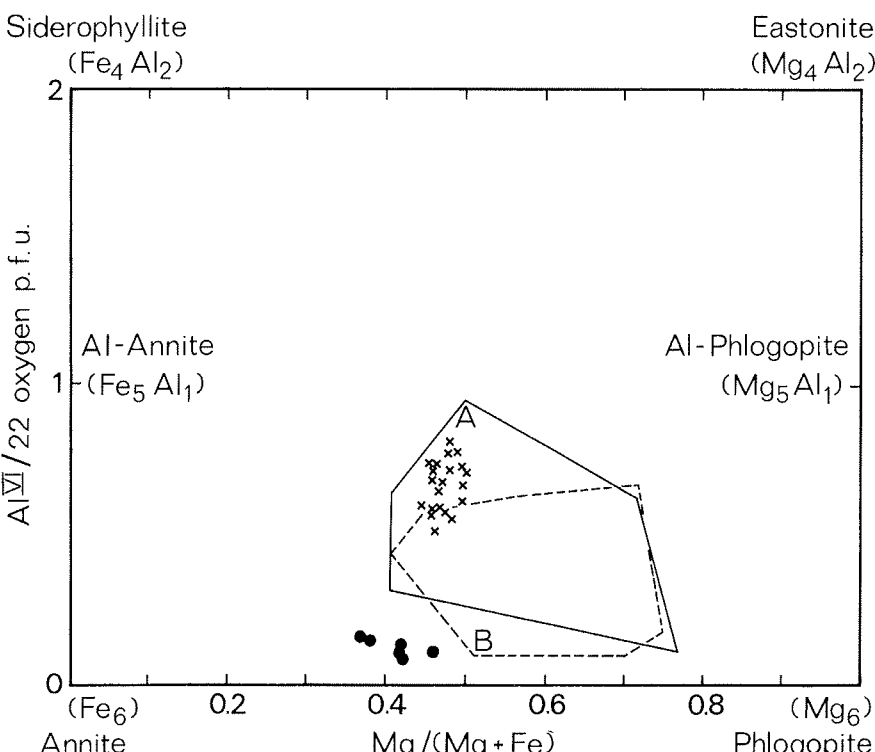


Fig. 7: Compositions of analyzed biotites in sillimanite-garnet-cordierite gneiss (crosses) from Hatch Plain compared with biotites in neighbouring enderbitic granulite (dots) plotted in the ideal Biotite-ebele Annite-Phlogopit-Siderophyllit-Eastonit. Field A (solid line) represents biotite from amphibolite- to granulite-grade metapelites, field B (dashed line) represents biotite compositions from granulite-grade metapelites according to GUIDOTTI (1984).

Abb. 7: Zusammensetzung der Biotite in Sillimanit-Granat-Cordieritgneisen von Hatch Plain (Kreuze), verglichen mit Biotiten benachbarter enderbitischer Granulite (Punkte), dargestellt in der idealen Biotiteebene Annit-Phlogopit-Siderophyllit-Eastonit. Das Feld A (durchgezogene Linie) umschließt Biotitzusammensetzungen aus amphibolit- bis granulitfaziellen Metapeliten, das Feld B (unterbrochene Linie) ein solches für Biotite aus rein granulitfaziellen Metapeliten nach GUIDOTTI (1984).

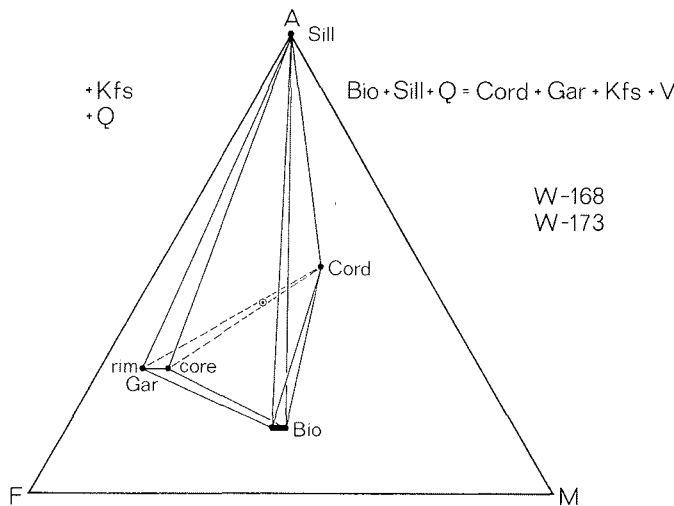


Fig. 8: AFM diagramm (projektiert durch Kalifeldspat) für koexistierende Mineralfaschen der Sillimanit-Granat-Cordieritegneise, Proben W-168 und W-173. Der Granatzonarbau wird durch Kern- und Randzusammensetzung markiert. Für die unzonierten Biotite wird der Zusammensetzungsbereich angegeben. Die unterbrochenen Konoden zwischen Granat und Cordierit markieren ein räumliches Subtetraeder, welches die stabile 4-Phasen-Vergesellschaftung Sillimanit-Granat-Cordierit-Biotit repräsentiert. Der unterbrochene Kreis stellt die Gesamtgesteinss Zusammensetzung der Probe W-173 dar.

Abb. 8: AFM-Diagramm (Projektion durch Kalifeldspat) der koexistierenden Mineralphasen der Sillimanit-Granat-Cordieritegneise, Proben W-168 und W-173. Der Granatzonarbau wird durch Kern- und Randzusammensetzung markiert. Für die unzonierten Biotite wird der Zusammensetzungsbereich angegeben. Die unterbrochenen Konoden zwischen Granat und Cordierit markieren ein räumliches Subtetraeder, welches die stabile 4-Phasen-Vergesellschaftung Sillimanit-Granat-Cordierit-Biotit repräsentiert. Der unterbrochene Kreis stellt die Gesamtgesteinss Zusammensetzung der Probe W-173 dar.

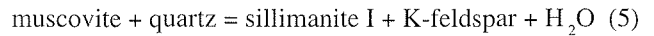
As emphasized in the petrographical section, sillimanite is observed to be partly still in contact with biotite (Fig. 5). In the AFM plot, this is demonstrated by the biotite-sillimanite tie-line. On the other hand, numerous inclusions of relict sillimanite needles in garnet and cordierite (Figs. 3 and 4) lack direct contact with biotite. This means that both the garnet- and the cordierite-forming reactions (1) and (2), respectively, moved completely to the mineral assemblage on the right, i.e. garnet + cordierite + K-feldspar + H_2O .

The garnet-cordierite tie-line connecting the two 3-phase fields sillimanite-garnet-cordierite and garnet-cordierite-biotite in the AFM plot is based on reactions (1) and (2). Because the widely present 4-phase assemblage sillimanite-garnet-cordierite-biotite of the garnet-cordierite gneiss forms a tetrahedron, the apparent intersection of the garnet-cordierite tie-line with the sillimanite-biotite tie-line visible in Fig. 8 is only an artifact of projection. The fifth component of the system, H_2O , is not shown in the figure. It would bring the projection point of biotite up to the H_2O corner, modifying the sillimanite-garnet-cordierite-biotite subtetrahedron to a 4-phase space.

It is interesting to note that in Fig. 8 the bulk rock composition of sample W-173 plots between the tie-line joining cordierite and garnet cores and that between cordierite and garnet rims. This could support the petrogenetic stability of the four-phase assemblage mentioned above over a relatively broad P-T range.

METAMORPHIC CONDITIONS

The general conditions are illustrated in Figs. 9 and 10. Neither kyanite nor andalusite were observed in the cordierite gneiss and migmatites from the Du Toit Nunataks, and sillimanite (sillimanite I and sillimanite II) is the only aluminum silicate recorded. The general absence of primary muscovite in the presence of quartz, sillimanite and K-feldspar indicates that the following sillimanite-producing reaction has taken place:



On the basis of field and microscopic observations, the stable mineral assemblage representing the peak of metamorphism is biotite + sillimanite + garnet (core) + cordierite + K-feldspar + plagioclase + quartz. This assemblage covers a relatively wide stability field, starting at about 550 °C and limited by dehydration reactions such as sillimanite + biotite + quartz = cordierite + garnet + K-feldspar + melt (ASHWORTH & CHINNER 1978, Fig. 1 and Equation. 2). As has already been mentioned, anatexic melting phenomena are well developed in the cordierite gneiss from the Du Toit Nunataks, documented by migmatitic structure with typical leucosome and melanosome.

In the petrogenetic grid (Fig. 10), a minimum pressure of 3.8 kb and a minimum temperature of 650 °C are thus indicated by the intersection of the univariant equilibrium curve (Equation 5) with the granite solidus, providing the fluid is essentially H_2O . An appreciable proportion of CO_2 in the fluid phase, for example, would shift the estimated minimum pressure and temperature to 5.6 kb/670 °C ($P\{H_2O\} = 0.7$; KERRICK 1972).

Geothermometry and geobarometry

Potential geothermometers are provided by the Mg-Fe partition between the mineral pairs garnet-biotite and garnet-cordierite. Opaque phases are scarce and usually associated with biotite retrogression; they have not been used for thermometry. Coexisting feldspars from the garnet-cordierite gneiss have not been used because of the uncertainties in obtaining bulk analyses of unexsolved and exsolved microcline, both of which probably have formed from inverted orthoclase.

The partition coefficients K_D^{Bi-Grt} and $K_D^{Crd-Grt}$ of the Mg-Fe exchange reactions between coexisting garnet-biotite and garnet-cordierite are a function of temperature. Garnet zoning is very pronounced and has already been discussed in terms of almandine-pyrope ratios; neighbouring biotite and cordierite, however, show no zoning. Following the argumentation of MARTINOLE & NANTEL (1982: 315), we can assume that the actual cordierite and biotite compositions are not significantly different from the composition during garnet core formation.

Pressure-independent garnet-biotite and garnet-cordierite thermometers have been modelled by THOMPSON (1976) and PERCHUK (1977). Application of these thermometers yields temperatures of 630-675 °C for the garnet core/biotite and garnet core/

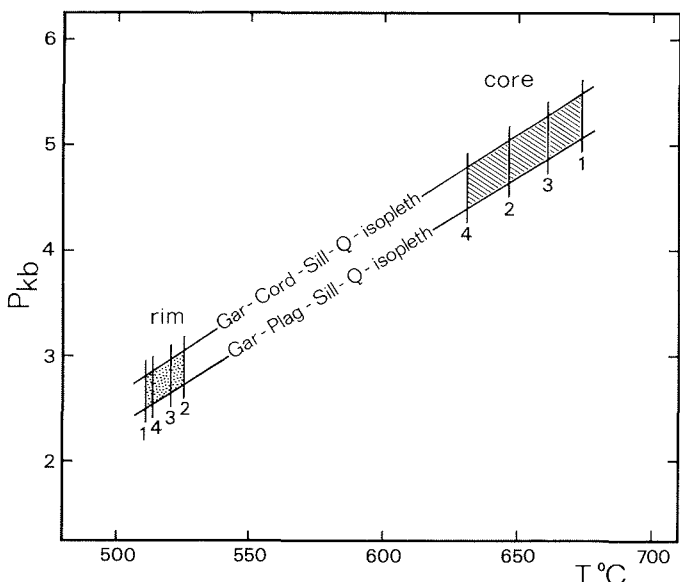


Fig. 9: Comparison of results using pressure-independent garnet-biotite thermometer calibrations of THOMPSON (1976) (1) and PERCHUK (1977) (2), and garnet-cordierite thermometer calibrations of THOMPSON (1976) (3) and PERCHUK (1977) (4) for representative garnet-biotite and garnet-cordierite pairs from sample W-173. In addition, the corresponding isopleths for garnet-plagioclase-sillimanite-quartz and for garnet-cordierite-sillimanite-quartz are shown using the pressure calibrations of GHENT et al. (1979) and PERCHUK et al. (1985), respectively.

Abb. 9: Vergleich der Ergebnisse der druckunabhängigen Granat-Biotit-Thermometer nach THOMPSON (1976) (1) und PERCHUK (1977) (2) und der Granat-Cordierit-Thermometer nach THOMPSON (1976) (3) und PERCHUK (1977) (4) für repräsentative Granat-Biotit- bzw. Granat-Cordierit-Paare aus Probe W-173. Zusätzlich sind die entsprechenden Isoplethen für die Barometer Granat-Plagioklas-Sillimanit-Quarz und Granat-Cordierit-Sillimanit-Quarz nach GHENT et al. (1979) bzw. PERCHUK et al. (1985) dargestellt.

cordierite relations, and 510–525 °C using garnet rim compositions, i.e. for the closure of exchange reactions (sample W-173, Tab. 3 and Fig. 9). Comparison of these thermometers shows a close correspondence of equilibration temperatures around 515 ± 10 °C and a relatively good correspondence around 650 °C.

On the basis of the well-documented stable four-phase assemblages garnet-plagioclase-sillimanite-quartz and garnet-cordierite-sillimanite-quartz, as well as of the independent temperature estimates, geobarometric calculations were made according to GHENT et al. (1979) and PERCHUK et al. (1985). These calculations indicate a maximum confining pressure of 5.5 ± 0.5 kb for the 650 ± 20 °C event (Fig. 9).

For a given K_D (Tab. 3), calculation of the pressure-dependent temperatures for the maximum pressure event according to FERRY & SPEAR (1978) results in temperatures 50–70 °C higher than those obtained by THOMPSON (1976) and PERCHUK (1977). As discussed in some detail by HARRIS & JAYARAM (1982), Ti and Al^{VI} of biotite reduce the accuracy of the thermometer. The maximum acceptable value for $(Al^{VI} + Ti)/(Al^{VI} + Ti + Fe + Mg)$ is 0.15 (FERRY & SPEAR 1978). The data of the analyzed biotites of Table 1 vary between 0.16–0.20, and typically less ideal biotites are the higher temperature phases.

In Fig. 10, P-T conditions of 515 °C and 2–3 kb indicated by the two mineral pairs garnet(rim)-biotite and garnet(rim)-cordierite fall in the chlorite-muscovite stability field, which petrographically is corroborated by the appearance of fine-grained secondary chorite and white mica in younger cracks in garnet (Fig. 4). It seems that late-kinematic sillimanite II still grew in the sillimanite stability field of the Al_2SiO_5 polymorphs, but this occurrence of sillimanite II possibly indicates a metastable situation on the andalusite side of the sillimanite-andalusite inversion curve, as discussed by KERRICK (1990).

Estimation of metamorphic trends

To determine the cooling and unloading history of the entire rock complex, grossular zoning in garnet, which is mainly pressure-dependent if developed in the presence of aluminum silicate + plagioclase + quartz, can be correlated with almandine-pyrope zoning, which is essentially temperature-dependent (MAARTIGNOLE & NANTEL 1982). In our samples, other minerals, e.g. plagioclase, biotite and cordierite, show no compositional variation with respect to X_{Ca} (indicating high-grade metamorphic conditions according to PERREAU & MARTIGNOLE 1988) and have not influenced X_{Ca} and X_{Mg} in garnet zoning. Thus, it is possible to use the covariation of X_{Ca} and X_{Mg} in garnet to monitor changing P-T conditions.

The correlation of Mg-Fe variations and Ca variations, as proposed by MARTIGNOLE & NANTEL (1982), is given in Fig. 11a. Although the grossular content of garnets from the garnet-cordierite gneiss of the Du Toit Nunataks is generally low ($Grs_{2.6-3.1}$), the trend defined by zonal compositional variation is systematic (Fig. 11b).

Pyrope-almandine garnets, the cores ($X_{Mg} = 0.17$) of which probably correspond to peak metamorphic temperatures, display a

Sample	Biotite	Cordierite	Garnet	$\ln K_D^*$	Garnet-Biotite			Garnet-Cord	
	Mg/Fe	Mg/Fe	Mg/Fe		Th	Pe	(F&S)	(Th)	(Pe)
W-173 core	0.864	1.665	0.222	2.024	674	647	729 (6 kb)	661	631
W-173 rim	0.893	1.665	0.128	2.585	511	525	503 (2.5 kb)	520	513
W-168 rim	0.941	1.559	0.136	2.435	514	529	502 (2.5 kb)	567	537

Tab. 3: Garnet-biotite and garnet-cordierite thermometry after THOMPSON (1976) = (Th), PERCHUK (1977) = (Pe) and FERRY & SPEAR (1978) = (F&S); temperature in °C. * $\ln K_D(Fe-Mg)$ for garnet-cordierite pairs according to THOMPSON (1976).

Tab. 3: Granat-Biotit und Granat-Cordierit Thermometrie nach THOMPSON (1976) = (Th), PERCHUK (1977) = (Pe) und FERRY & SPEAR (1978) = (F&S), Temperatur in °C.

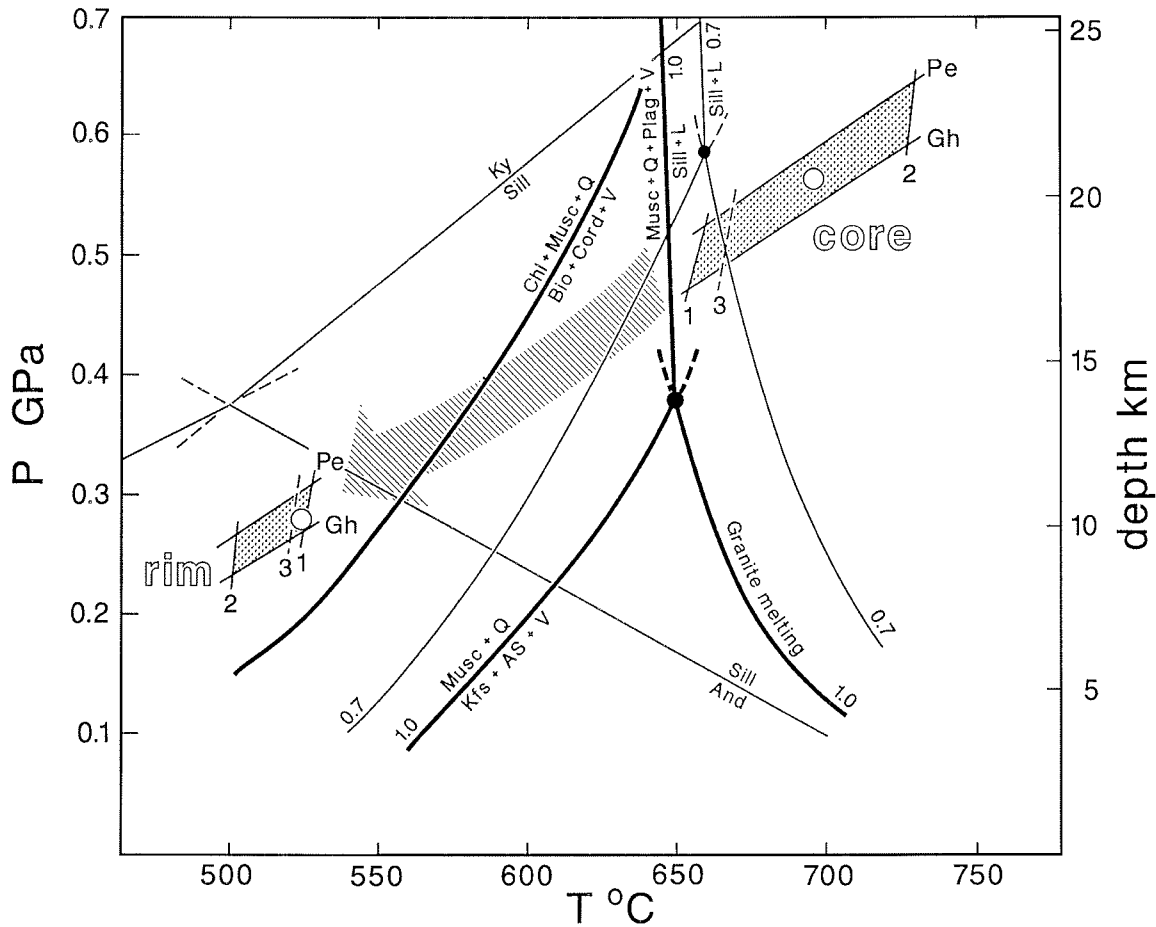


Fig. 10: $P(H_2O)$ - T conditions of metamorphism, based on mineral assemblages and mineral composition of representative sillimanite-garnet-cordierite gneiss W-173. Calculated temperatures of coexisting garnet and biotite are after (1) PERCHUK et al. (1985), (2) FERRY & SPEAR (1978); temperatures of coexisting garnet and cordierite are after (3) PERCHUK et al. (1985). Pressure estimates according to (Gh) GHENT et al. (1979), (Pe) PERCHUK et al. (1985). White dots mark the P and T calculations after ARANOVICH & PODLESSKII & (1983: Fig. 10). P-T conditons of garnet core and garnet rim are indicated. Chlorite+muscovite+quartz stability curve after BIRD & FAWCETT (1973); the muscovite+quartz stability curve (reaction 5), the granite melting curve, and the muscovite melting reaction curve emanating from the intersection of the first two curves at $P(H_2O) = 0.7$ and 1.0 are after KERRIK (1972). Aluminum silicates after HOLDAWAY (1971). The hatched area indicates the conditions of the main metamorphic event continuously shifting to lower P-T conditions by a process of unloading and cooling (see text), marked by the arrow. AS = andalusite or sillimanite.

Abb. 10: Druck-Temperatur-Bedingungen der Metamorphose basierend auf Mineralparagenese und Mineralchemismen des repräsentativen Sillimanit-Granat-Cordieritgneises W-173. Berechnete Temperaturen von koexistierendem Granat und Biotit nach (1) PERCHUK et al. (1985), (2) FERRY & SPEAR (1978); Temperaturn von koexistierender Granate und Cordierit nach (3) PERCHUK et al. (1985). Drucke nach (Gh) GHENT et al. (1979) und (Pe) PERCHUK et al. (1985). Weiße Kreise markieren die P-T-Berechnung nach ARANOVICH & PODLESSKII (1983, Fig. 10). P-T-Bedingungen für Granatkern- und Granatrandzusammensetzungen sind markiert. Stabilitätskurve Chlorit + Muskovit + Quarz nach BIRD & FAWCETT (1973); Stabilitätskurve Muskovit + Quarz, Granitschmelzkurve und die, am Schnittpunkt beider beginnende Kurve Muskovit + Quarz + Plagioklas + H_2O für $P(H_2O) = 0.7$ bzw. 1.0 nach KERRIK (1972). Stabilität der Aluminiumsilikate nach HOLDAWAY (1971). Das schraffierte Feld markiert die Hauptmetamophorebedingungen, welche sich zu niedrigeren P-T-Bedingungen hin durch Entlastung und Abkühlung verschieben (vgl. Text).

decrease in X_{Mg} towards the rim ($X_{Mg} = 0.11$), but show a nearly constant X_{Ca} value (Table 1). This observation corresponds to the type 2 pattern of MARTIGNOLE & NANTEL (1982: Fig. 3), characteristic for „cooling during unloading“. This combined process of cooling and unloading is further supported by the bell-shaped form of the zoning curves (Fig. 6), indicating steady garnet growth. Thus, a medium-pressure type of regional metamorphism under amphibolite facies conditions can be inferred for this central part of the metamorphic Proterozoic crust of the Shackleton Range. In the area under discussion, a geothermal gradient of about $32\text{ }^{\circ}\text{C/km}$ can be obtained for the time of the amphibolite facies tectonometamorphic event from petrological mineral equilibria.

CONCLUSIONS

This study provides new information about the metamorphic evolution of the gneiss-migmatite complex of the basement of the central Read Mountains (Read Group) based mostly on textural relations, on mineral equilibria, and on geothermobarometric calculations. Most of the Read Group rocks are paragneisses, migmatites, amphibolites, and marbles coupled with orthogneiss („granitic gneiss“) of Middle Proterozoic age according to the radiometric data of REX (1972) and PANKHURST et al. (1983).

The first occurrence of cordierite in the Shackleton Range was

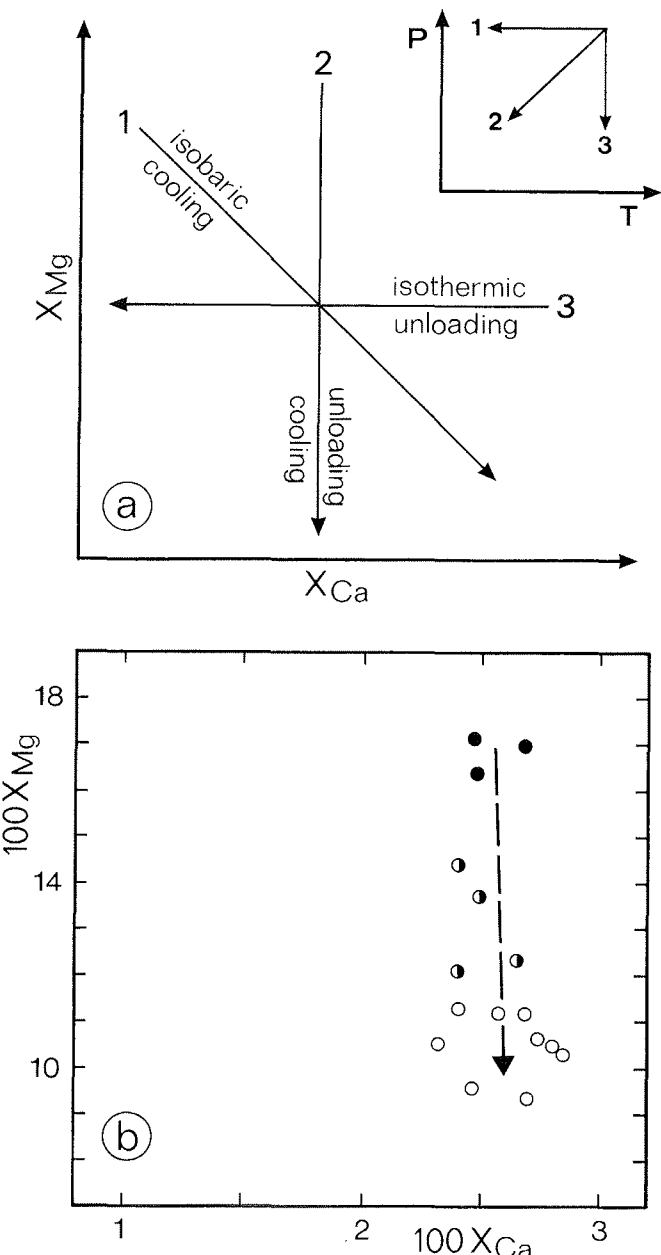


Fig. 11: (a) Interpretation of garnet zoning in terms of evolving P-T conditions after MARTIGNOLE & NANTEL (1982). (b) Analyzed garnets of sillimanite-garnet-cordierite gneiss samples W-168 and W-173 from Hatch Plain, Du Toit Nunataks in the Read Mountains. Filled circles: cores of garnet; half-filled circles: halfway between core and rim of garnets; open circles: rim of garnets. See text for explanation.

Abb. 11: (a) Interpretation von Granatzonarbau und sich ändernden P-T-Bedingungen nach MATIGNOLE & NANTEL (1982). (b) Analysierte Granate aus Sillimanit-Granat-Cordieritgneis, Proben W-168 und W-173 von Hatch Plain, Du Toit Nunataks, Read Mountains. Gefüllte Kreise = Granatkerne, halbfüllte Kreise = Mittelbereiche zwischen Granatkern und Granatrand, offene Kreise = Granatränder. Weitere Erläuterungen siehe Text.

recognized within the gneiss-migmatite complex from Hatch Plain in the Du Toit Nunataks. It is in sillimanite-garnet-cordierite-bearing parts of the melanosomic portions of metatectic and migmatitic rocks. Petrological phase analyses of the cordierite-garnet-sillimanite-K-feldspar-quartz assemblage reveals that both garnet and cordierite were formed by prograde mineral reactions.

Geothermometry using coexisting garnet-cordierite-biotite and geobarometry using garnet-plagioclase/cordierite-sillimanite-quartz yield equilibrium temperatures of about 690 °C at 5-6 kb confining pressure. Together with well-documented migmatization phenomena, the evaluated pressure and temperature indicate amphibolite facies conditions for the main metamorphic event, followed by uplift with cooling and unloading down to 2-3 kb P(H₂O). Similar conditions of 2.2 kb at 610 °C were obtained by SCHULZE (1989) for the associated gneissic granite, indicating a common final low-pressure history.

Relict enderbitic granulite associated with amphibolites of Hatch Plain (Fig. 2) reveals pressure-temperature conditions of about 8 kb and 760 °C, using new mineral data of garnet, orthopyroxene, biotite, plagioclase and the calibration models of BOHLEN et al. (1983) and GANGULY & SAXENA (1984). These P-T conditions given by the enderbitic granulite of the Read Mountains basement are comparable with similar low-pressure granulites from other parts of the East Antarctic craton (GREW 1981).

The evaluated low-pressure granulite conditions of Hatch Plain are suggested to have resulted either from under-accretion (WELLS 1979), indicated by a relatively high geothermal gradient (BOHLEN et al. 1983) or during a phase in which the conditions were reset between granulite and amphibolite facies. On the other hand, SCHULZE & OLESCH (1990) described relic granulite facies rocks from the Read Mountains basement, which are characterized by higher pressures between 8-12 kb at relatively low temperatures of 540-620 °C, thus indicating a Proterozoic crustal thickness of at least 40 km. The observed high pressures at relatively low temperatures and the nearly isothermal uplift are understandable only if a specific geodynamic model is used.

The following scenario is suggested, which is a modified version of the model of CUTHBERT et al. (1983). After initial subduction, a subsequent collision creates a multiple imbrication zone with crustal thickening. The isotherms within the crust represent relatively low temperatures due to the influence of subducted cooler material. Metamorphism occurs, therefore, under high pressure, but relatively low temperature (see also ENGLAND & THOMPSON 1984, BOHLEN 1991). Before thermal relaxation takes place, the collision continues by underthrusting one or more cold slabs. Owing to isostatic conditions, the metamorphic rocks are uplifted without having suffered any high temperatures. This model explains the path of pressure and temperature of the granulitic metamorphics of the central and easternmost Read Mountains. In addition, the existence of a collision zone in this area during the Late Proterozoic is implied.

Correlation of structural data of BRAUN (1992) with available geochronological data (PANKHURST et al. 1982, HOFMANN & PAECH 1983) indicates a pre-D₁ tectonometamorphic event, presumably under granulite facies conditions at 2200 Ma and a D₁ tectonometamorphic event under amphibolite facies conditions in the time span of 1640-1420 Ma, passing into the low-pressure retrogression.

ACKNOWLEDGEMENTS

This study was part of the mineralogical and petrological research conducted by the Geological Expedition to the Shackleton Range Antarctica „GEISHA 1987/88“. We are grateful to the Deutsche Forschungsgemeinschaft Bonn (DFG) for grants to the authors. Extensive logistical support of the field work from the Alfred-Wegener-Institut für Polarforschung, Bremerhaven (AWI), from the Bundesanstalt für Geowissenschaften und Rohstoffe, Hannover (BGR), and from the British Antarctic Survey, Cambridge (BAS) is gratefully acknowledged. We thank all our colleagues for help and fruitful discussions in the field and during the work after the expedition. The criticism and comments by H.-M. Braun on an early version of the manuscript were most helpful.

References

- Aranovich, L.Y. & Podlesskii, K.K. (1983): The cordierite-garnet-sillimanite-quartz equilibrium: experiments and applications.- In: S.K. SAXENA (Ed.), Advances in Physical Geochemistry, Vol. 3: Kinetics and equilibrium in mineral reactions, 173-198, Springer Verlag, Berlin.
- Armbruster, T. & Bloss, F.D. (1982): Orientation and effects of channel H_2O and CO_2 in cordierite.- Amer. Miner. 67: 284-291.
- Ashworth, J.R. & Chinner, G.A. (1978): Coexisting garnet and cordierite in migmatites from the Scottish Caledonides.- Contr. Miner. Petrol. 65: 379-394.
- Bird, G.W. & Fawcett, J.J. (1973): Stability relations of Mg-chlorite, muscovite and quartz between 5 and 10 kb water pressure.- J. Petrol. 14: 415-428.
- Blümel, P. (1978): Die Bedeutung kontinuierlicher und diskontinuierlicher Mineralreaktionen als PT-Indikatoren der Metamorphose im prä-permischen Kristallin Süddeutschlands.- Zeitschr. dt. Geol. Ges. 129: 359-375, Hannover.
- Blümel, P. & Schreyer W. (1977): Phase relations in pelitic and psammitic gneisses of the sillimanite-potash feldspar and cordierite-potash feldspar zones in the Moldanubicum of the Lam-Bodenmais area, Bavaria.- J. Petrol. 18: 431-459.
- Bohlen, S.R. (1991): On the formation of granulites.- J. Metam. Geol. 9: 223-229.
- Bohlen, S.R., Wall, V.J. & Boettcher, A.L. (1983): Experimental investigation and application of garnet granulite equilibria.- Contr. Miner. Petrol. 83: 52-61.
- Braun, H.-M. (1992): Strukturgeologische Untersuchungen im kristallinen Grundgebirge der Shackleton Range, Antarktis.- Unpubl. Diss. Univ. Frankfurt.
- Clarkson, P.D. (1972): Geology of the Shackleton Range: a preliminary report.- Brit. Antarct. Surv. Bull. 31: 1-15.
- Clarkson, P.D. (1982): Geology of the Shackleton Range: I. The Shackleton Range Metamorphic Complex.- Brit. Antarct. Surv. Bull. 51: 257-283.
- Cuthbert, S.J., Harvey, M.A. & Carswell, D.A. (1983): A tectonic model for the metamorphic evolution of the Basal Gneiss Complex, West South Norway.- J. Metam. Geol. 1: 63-90.
- Dymek, R.F. (1983): Titanium, aluminum, and interlayer cation substitution in biotite from high grade gneisses, West Greenland.- Amer. Miner. 68: 880-899.
- England, P.C. & Thompson, A.B. (1984): Pressure-temperature-time paths of regional metamorphism I. Heat transfer during the evolution of regions of thickened continental crust.- J. Petrol. 25: 894-928.
- Ferry, J.M. & Spear, F.S. (1978): Experimental calibration of the partitioning of Fe and Mg between garnet and biotite.- Contr. Miner. Petrol. 66: 113-117.
- Ganguly, J. & Saxena, S.K. (1984): Mixing properties of alumino-silicate garnets: constraints from natural and experimental data and applications to geothermobarometry.- Amer. Miner. 69: 88-97.
- Ghent, E.D. & Robbins, D.B. & Stout, M.Z. (1979): Geothermometry, geobarometry, and fluid compositions of metamorphosed calcsilicates and pelites, Mica Creek, British Columbia.- Amer. Miner. 64: 874-885.
- Grew, E.S. (1981): Granulite-facies metamorphism at Molodezhnaya Station, East Antarctica.- J. Petrol. 22: 297-336.
- Guidotti, Ch.V. (1984): Micas in metamorphic rocks.- In: S. BAILEY (Ed.): Micas, Reviews in Mineralogy 13, 357-468, Miner. Soc. America.
- Harris, N.B.W. & Jayaram, S. (1982): Metamorphism of cordierite gneisses from the Bangalore region of the Indian Archean.- Lithos 15: 89-98.
- Hofmann, J. & Paech, H.-J. (1983): Tectonics and relationships between structural stages in the Precambrian of the Shackleton Range, Western margin of the East Antarctic Craton.- In: R.L. Oliver, P.R. JAMES & J.B. JAGO, (Eds.), Antarctic Earth Science, Austral. Acad. Sci., 183-189, Canberra.
- Holdaway, M.J. (1971): Stability of andalusite and the aluminum silicate phase diagram.- Amer. J. Sci. 271: 97-131.
- Kerrick, D.M. (1972): Experimental determination of muscovite + quartz stability with $P_{H2O} < P_{total}$.- Amer. J. Sci. 272: 946-958.
- Kerrick, D.M. (1990): The Al_2SiO_5 polymorphs.- Reviews in Mineralogy 22, pp. 406.
- Martignole, J. & Nantel, S. (1982): Geothermobarometry of cordierite-bearing metapelites near the Morin anorthosite complex, Grenville Province, Quebec.- Canad. Miner. 20: 307-318.
- Pankhurst, R.J., Marsh, P.D. & Clarkson, P.D. (1983): A geochronological investigation of the Shackleton Range.- In: R.L. OLIVER, P.R. JAMES & J.B. JAGO (Eds.), Antarctic Earth Science, Austral. Acad. Sci., 176-182, Canberra.
- Perchuk, L.L. (1977): Thermodynamic control of metamorphic processes.- In: S.K. SAXENA & S. BHATTACHARJI (Eds.), Energetics of Geological Processes, 286-352, Springer Verlag, Berlin.
- Perchuk, L.L., Aranovich, L.Y., Podlesskii, K.K., Lavrent'eva, I.V., Gerasimov, V.Y., Fed'kin, V.V., Kitsul, V.I., Karkasov, L.P. & Berednikov, N.V. (1985): Precambrian granulites of the Aldan shield, eastern Siberia, USSR.- J. Metam. Geol. 3: 265-310.
- Perreault, S. & Martignole, E.J. (1988): High-temperature cordierite migmatites in the north-eastern Grenville Province.- J. Metam. Geol. 6: 673-696.
- Raheim, A. (1975): Mineral zoning as a record of P,T history of Precambrian eclogites and schists in western Tasmania.- Lithos 8: 231-236.
- Rex, D.C. (1972): K-Ar age determinations on volcanic and associated rocks from the Antarctic Peninsula and Dronning Maud Land.- In: R.J. ADIE (Ed.), Antarctic Geology and Geophysics, 133-136, Oslo, Universitetsforlaget.
- Schubert, W. & Will, T. (1994): Granulite-facies rocks of the Shackleton Range, Antarctica. Conditions of formation and preliminary petrogenetic implications. - Chemie Erde 54: 355-371.
- Schulze, P. (1989): Petrographie und Petrogenese der Gesteine von Beche Blaude (Read Mountains) und Unnamed Nunatak (SSW Meade Nunatak, Pioneers Escarpment), Shackleton Range, Antarktis.- Unpubl. Dipl.-Arb., Miner. Inst. Univ. Würzburg, pp. 123.
- Schulze, P. & Olesch, M. (1990): Granulitfazielle Relikte im Pioneers Escarpment, Shackleton Range, Antarktis.- Europ. J. Miner. 2, Beih. 1: 234.
- Thompson, A.B. (1976): Mineral reactions in pelitic rocks. II Calculation of some P-T-X (Fe-Mg) phase relations.- Amer. J. Sci. 276: 425-454.
- U.S. Geological Survey (1983): 1 : 250 000 map of Antarctica.- U.S. Geol. Surv. Reconnaissance Series, SU 26-30/1.
- Wells, P.R.A. (1979): Chemical and thermal evolution of Archaean sialic crust, Southern West Greenland.- J. Petrol. 20: 187-226.
- Wimmenauer, W. (1984): Das prävariskische Kristallin im Schwarzwald.- Fortschr. Miner. 62, Beih. 2: 69-86.
- Winkler, H.G.F. (1979): Petrogenesis of metamorphic rocks, 5. ed., pp. 348, Springer Verlag, New York, Heidelberg, Berlin.
- Young, E.D., Anderson, J.L., Clarke, H.S. & Thomas, W.M. (1989): Petrology of biotite-cordierite-garnet gneiss of the McCullough Range, Nevada. I. Evidence for Proterozoic low-pressure fluid-absent granulite-grade metamorphism in the Southern Cordillera.- J. Petrol. 30: 39-60.